ARTICLE

Hierarchy of orofacial rhythms revealed through whisking and breathing

Jeffrey D. Moore[1]*, Martin Deschênes[2]*, Takahiro Furuta[3], Daniel Huber[4]†, Matthew C. Smear[4], Maxime Demers[2] & David Kleinfeld[1,5]

Whisking and sniffing are predominant aspects of exploratory behaviour in rodents. Yet the neural mechanisms that generate and coordinate these and other orofacial motor patterns remain largely uncharacterized. Here we use anatomical, behavioural, electrophysiological and pharmacological tools to show that whisking and sniffing are coordinated by respiratory centres in the ventral medulla. We delineate a distinct region in the ventral medulla that provides rhythmic input to the facial motor neurons that drive protraction of the vibrissae. Neuronal output from this region is reset at each inspiration by direct input from the pre-Bötzinger complex, such that high-frequency sniffing has a one-to-one relationship with whisking, whereas basal respiration is accompanied by intervening whisks that occur between breaths. We conjecture that the respiratory nuclei, which project to other premotor regions for oral and facial control, function as a master clock for behaviours that coordinate with breathing.

Active sensing is an essential component of orofacial behaviour. Animals rhythmically sniff to smell, lick to taste, and whisk to touch. The muscles involved in these patterned sensory behaviours overlap with those involved with the ingestive behaviours of chewing, swallowing and suckling. Notably, all of these behaviours share the motor plant involved in respiration and control of the upper airway. Given the essential nature of breathing and the biomechanical constraints that link the different behaviours, the coordination among orofacial behaviours constitutes a computational aspect of homeostatic control with little margin for error[1–6].

Here we investigate the coordination of orofacial behaviours in the context of sniffing and whisking in rodents. These closely associated rhythmic behaviours constitute the animals' predominant activities during exploration and social interactions[7–9]. The cycle of rhythmic breathing is driven by neurons in the pre-Bötzinger complex, which generates the inspiratory rhythm[10,11], the Bötzinger complex and parafacial respiratory groups, which shape the expiratory rhythm[5], the ventral respiratory groups, which drive the respiratory pump muscles[12], and several pools of cranial motor neurons that control the upper airway valve muscles[13]. The drive for rhythmic whisking remains to be identified. However, whisking persists after decortication[7,14] and sensory deafferentation[7,15,16], which suggests that it too involves a rhythmic generator in the brainstem. Furthermore, the facial motor neurons that drive the muscles involved in whisking are located immediately rostral to nuclei within the ventral medulla that generate breathing, and activity within these facial motor neurons and muscles is time-locked to breathing[17,18]. These results reported previously support a common neural circuitry for the rhythmic control of both breathing and whisking.

Obligatory phase-locking of whisking and breathing

Concurrent measurements of breathing and whisking in head-fixed rats reveal key aspects of their coordination (Fig. 1a, b). First, breathing over a wide range of rates can occur without substantial whisking
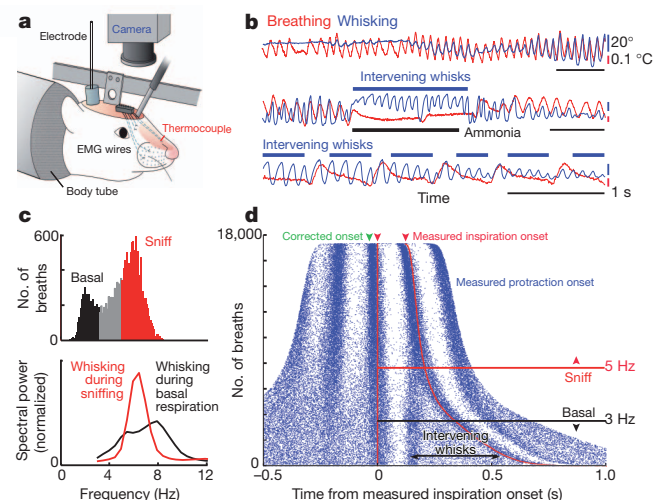

Figure 1 | Coordination of whisking and breathing. a, Procedures to measure whisking, breathing and associated electrophysiology in head-restrained rats. **b**, Simultaneous measurement of vibrissa position (blue) and breathing (red). Protraction and inspiration are upwards. **c**, Histogram of instantaneous breathing frequencies (top) delineates the classification of breaths below 3 Hz as basal respiration (black) and those above 5 Hz as sniffs (red); unclassified frequencies are in grey. The spectral power of whisking (bottom) is plotted during periods of basal respiration (black) as well as sniffing (red). **d**, Raster plots of inspiration onset times (red) and protraction onset times (blue) relative to the onset of inspiration for individual breaths are ordered by the duration of the breath; green arrow represents the 30-ms lead of inspiratory drive to facial muscles as opposed to the measured inspiration. Whisks and inspiration onset times are significantly correlated during both sniffing and basal respiration ($P < 0.01$).

[1]Department of Physics, University of California at San Diego, 9500 Gilman Drive, La Jolla, California 92093, USA. [2]Department of Psychiatry and Neuroscience, Centre de Recherche Université Laval Robert-Giffard, 2601 de la Canardière, Québec City G1J 2G3, Canada. [3]Department of Morphological Brain Science, Building C Room 204, Graduate School of Medicine, Kyoto University, Yoshida Konoe-cho, Sakyo-ku, Kyoto 606-8501, Japan. [4]Howard Hughes Medical Institute, Janelia Farm Research Campus, 19700 Helix Drive, Ashburn, Virginia 20147, USA. [5]Section on Neurobiology, University of California at San Diego, 9500 Gilman Drive, La Jolla, California 92093, USA. †Present address: Department of Neuroscience, 1, rue Michel Street, University of Geneva, 1206 Geneva, Switzerland.
*These authors contributed equally to this work.

(Fig. 1b). To test whether whisking can also occur without breathing, we applied a puff of ammonia to the snout, which inactivates the central inspiratory drive[19] (Supplementary Fig. 1) and temporarily inhibits respiration. Critically, rats can whisk during such a disruption in breathing (Fig. 1b), which implies that the oscillator (or oscillators) for breathing and whisking are separately gated.

Exploratory behaviour typically consists of bouts of simultaneous whisking and fast breathing, or 'sniffing'[7]. Under such circumstances, fast breathing has a one-to-one relationship with whisking (that is, each breath is associated with a whisk) (Fig. 1b), which is clearly evident as the rat begins to breathe again after apnea (Fig. 1b). In contrast, basal breathing is accompanied by whisks that are coincident with an inspiration, termed 'inspiratory whisks', and with decrementing 'intervening whisks' that occur between successive breaths (Fig. 1b). This leads to an incommensurate relationship between whisking and breathing, with multiple whisks between breaths. These data imply that there are separate, or separable, oscillators for breathing and whisking, and that the breathing rhythm may reset the whisking rhythm.

The temporal relationship between whisking and breathing was quantified across the complete data set (five rats) (Fig. 1c, d). We observe that breathing occurs over a broad range of frequencies, but has two modes (Fig. 1c). We define 'basal respiration' as epochs with a breathing rate that is below 3 Hz, and 'sniffing' as epochs with rates that are higher than 5 Hz (Fig. 1c). Whisking has a broad, high-frequency spectral content during both basal respiration and sniffing (Fig. 1c). The detailed timing between whisking and breathing is revealed though a frequency-ordered plot of the correlation of whisking with breathing (Fig. 1d). Vibrissa protractions are time-locked to the onset of inspiration across the entire range of breathing frequencies; the green arrow in Fig. 1d accounts for the delay between inspiratory drive to diaphragm relative to that of the upper airway[20]. Basal respiration cycles are accompanied by multiple whisks per breath, with an instantaneous whisking frequency of approximately 8 Hz for the intervening whisks (Figs 1d and Supplementary Fig. 2). Analogous results, but with an instantaneous whisking frequency of approximately 13 Hz for the intervening whisks, are observed with mice ($n = 4$) (Supplementary Fig. 3). Lastly, phase-sensitivity analysis[21] shows that inspirations late in the whisk cycle elicit a new protraction earlier than expected (Supplementary Fig. 4) and that breathing drives whisking but not vice versa (Supplementary Fig. 5). Collectively, these data imply a unidirectional connection from the breathing oscillator[5,6,10] to a still hypothetical oscillator that generates whisking.

Facial muscles involved in whisking and breathing

Whisking and breathing-associated nose movements share facial muscle groups[22–24]. Thus, the difference in the pattern of whisking versus basal respiration (Fig. 1b) raises the issue of which muscle groups follow the sequence of motor commands associated with whisking[25] as opposed to those associated with breathing[1]. In particular, protraction of the vibrissae is driven primarily by intrinsic papillary muscles that wrap around the individual vibrissa follicles (Fig. 2a), whereas retraction involves viscoelastic forces as well as translation of the mystacial pad[15] that is driven by the 'extrinsic' nasolabialis and maxillolabialis muscles[25] (Fig. 2a). This determination of motor control is essential to understand the premotor brainstem circuits that drive different aspects of whisking.

We observe that the activity of the intrinsic muscles, measured from their differential electromyogram (∇EMG), leads protraction for both sniffing (Fig. 2b) and basal respiration (Fig. 2c). The nasolabialis muscle, also measured from its ∇EMG, is active for every whisk during sniffing (Fig. 2b) but is only active for inspiratory whisks during basal breathing (Fig. 2c). The timing and extent of this process was quantified in terms of the population averaged cross-correlations between the different features of whisking and the $|\nabla$EMG$|$ of the different muscle groups (3,600 inspiratory and 500 intervening whisks in two rats). This analysis indicates that there is consistent modulation
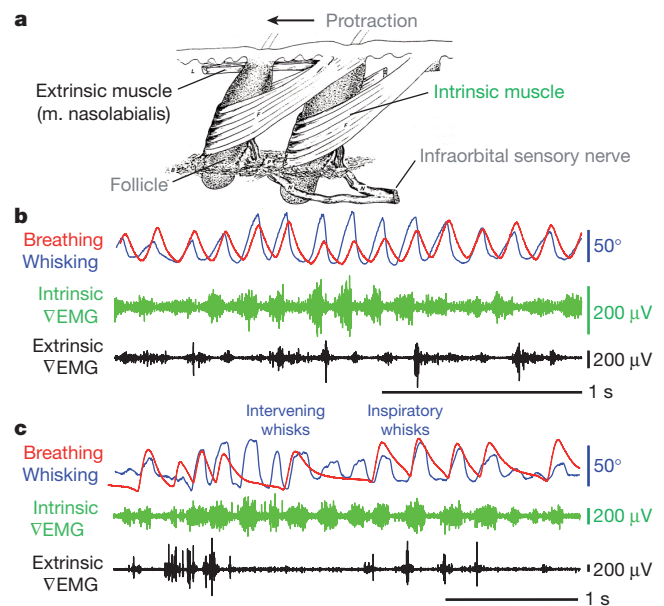

Figure 2 | Facial muscle activity during whisking and breathing. a, The musculature responsible for vibrissa and mystacial pad motion (adapted from a study published previously[24]). **b**, Vibrissa motion, breathing, and intrinsic and extrinsic ∇EMG activity during whisking and sniffing. **c**, The same activity during whisking and mixed basal respiration and sniffing.

of the intrinsic $|\nabla$EMG$|$ during both inspiratory and intervening whisks but that modulation of the extrinsic $|\nabla$EMG$|$ activity only occurs during inspiratory whisks (Supplementary Fig. 6), thus providing information that adds to our understanding of the role of extrinsic muscles gained from previous studies[15,25]. These data imply that protraction is driven by the proposed whisking oscillator, whereas retraction of the mystacial pad is at least partly controlled by respiratory patterning circuitry.

Identification of a region that signals whisking

The coordination of whisking with breathing, and the resetting of whisking by inspiration, suggest that a vibrissa pattern generator is driven by respiratory nuclei, which are known to lie in the ventral medulla[1]. Furthermore, the differences in the basal respiration and whisking patterns provides a signature to discriminate between breathing and potential whisking neuronal centres (Fig. 1b). We recorded multi-unit spiking activity in the area of the pre-Bötzinger, Bötzinger and adjoining ventral and parafacial respiratory regions (Fig. 3a–c), and identified each recording site by the location of a fiducial in a subsequent reconstruction of the brainstem (Fig. 3d, e). The functional attributes of each multi-unit signal were categorized as inspiratory or protractive (32 units), expiratory or retractive (29 units), or whisking (5 units) based on their patterns of activity during whisking and sniffing (Fig. 3f). We find that units that have a similar phase preference also lie in close spatial proximity (Fig. 3d–f). Specifically, multi-unit activity in the region of the pre-Bötzinger complex and the ventral respiratory group occurred in phase with inspiration and protraction of inspiratory whisks (Fig. 3a, d, e). Multi-unit activity in the region of the Bötzinger complex and the parafacial respiratory group occurred in approximate phase with expiration and retraction of inspiratory whisks (Fig. 3b, d, e). In both cases the activity did not track the intervening whisks. In contrast, we located a subset of units in the intermediate band of the reticular formation (IRt) whose spiking was tightly phase-locked to the protraction of both inspiratory and intervening whisks (Figs 3c and Supplementary Fig. 7). These units are potential premotor drivers of the intrinsic muscles that serve rhythmic whisking (Fig. 2a) and are henceforth referred to as 'whisking units'. They are located in the ventral part of the IRt, medial to the ambiguus nucleus
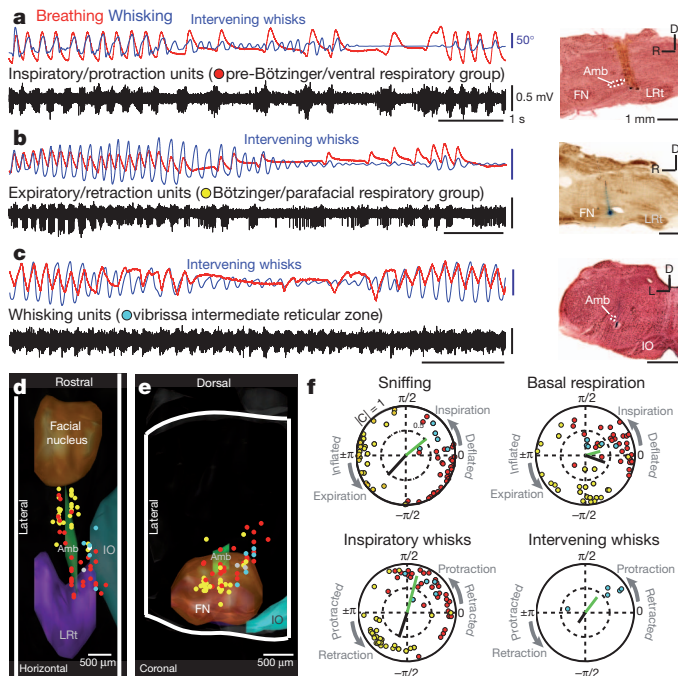
Figure 3 | **Activity in medullary respiratory centres during breathing and whisking. a**, Concurrent recordings of breathing (red), whisking (blue), and multiunit activity (black) in the pre-Bötzinger complex. The location of the recording site is labelled with Chicago sky blue and is shown in a sagittal section counterstained with neutral red. Amb, nucleus ambiguus; D, dorsal; FN, facial nucleus; IO, inferior olive; L, lateral; LRt, lateral reticular nucleus; R, rostral. **b**, Multi-unit spike activity in the Bötzinger complex. The section is counterstained for cytochrome oxidase. **c**, Multi-unit spike activity in the vibrissa zone of the intermediate reticular formation. The section is counterstained with neutral red. **d**, **e**, The recording sites for all data, indicated by coloured dots in panels **a** to **c**, imposed on a three-dimensional reconstruction of the medulla. Whisking units are located dorsomedially to the pre-Bötzinger complex in the IRt. Two units whose spiking had no relation to breathing or whisking are shown in white. White lines are tissue boundaries or limits of the reconstruction. **f**, Polar plots of the magnitude (0 to 1 radial coordinate) and phase (angular coordinate) of the coherence between multiunit spiking activity and measured behaviours at the peak frequency for each behaviour; that is, 2 Hz for basal respiration, 6 Hz for sniffing and inspiratory whisks, and 8 Hz for intervening whisks (Fig. 1c). Only units with significant coherence ($P < 0.01$) are shown and correspond to the points in panels **d** and **e**. The coherence (C), between the measured behaviour and the ∇EMG of the intrinsic muscles (green bar) and nasolabialis muscle ∇EMG (black bar) are shown.

pars semicompacta and near the pre-Bötzinger complex (Fig. 3d, e). We denote this new region the vibrissa zone of the IRt (vIRt).

The phase of the neuronal activity of the above three classes of rhythmically spiking units with respect to behaviour was compared with that of the intrinsic and nasolabialis |∇EMG| (Fig. 3f). First, there is a slight phase lead between the majority of whisking units and the intrinsic muscles. Second, the activity of inspiratory or protraction units tends to lead that of the whisking units, which is particularly robust during near synchronous whisking and sniffing (Fig. 3f). These data are consistent with inspiratory or protraction units located in or near the pre-Bötzinger complex resetting a group of rhythmic whisking units in the IRt to initiate protraction. In addition, expiratory or retraction units show a phase shift between sniffing and basal respiration that is paralleled by a concurrent shift in activation of the nasolabialis muscle (Fig. 3f).

Activation of the vIRt induces whisking

The hypothesis that whisking in the vIRt constitutes the oscillator for whisking predicts that activation of this region will lead to prolonged autonomous activity. Indeed, microinjection of the glutamate receptor

agonist kainic acid in the vicinity of the vIRt is a robust means to induce prolonged rhythmic muscular activation (Fig. 4a and Supplementary Fig. 8) and coordinated vibrissa protraction (Supplementary Fig. 9), near 10 Hz, in the lightly anaesthetized head-fixed rat (Fig. 4b and Supplementary Video 1). The frequency of whisking decreases over time, and the amplitude increases, as the effect of anaesthesia declines, whereas the frequency of breathing remains constant (Fig. 4b). This implies that the chemical activation is sufficiently strong to decouple rhythmic protraction from breathing (Supplementary Fig. 10). Quantitatively, the modulation depth of protraction with breathing was less than 0.01 and insignificant for all but one case (11 epochs for three rats), compared with 0.08 for basal respiration and 0.26 for sniffing in awake animals. Finally, consistent with the conclusions from the EMG studies (Supplementary Fig. 6), the mystacial pad moves in synchrony with breathing (Fig. 4a).

Chemical activation of rhythmic whisking, with a frequency incommensurate with that of breathing, provides an opportunity to stably record from units whose firing times were coherent with rhythmic protraction (Fig. 4c). We identified units that spiked in synchrony
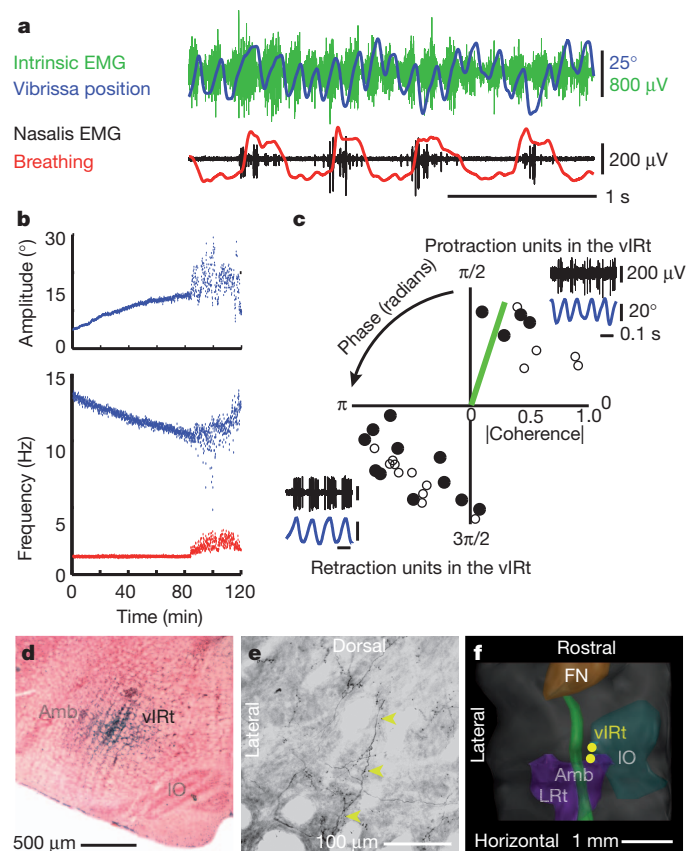

Figure 4 | **Injection of kainic acid in the medullary reticular formation induces whisking. a**, Vibrissa motion, breathing, intrinsic and extrinsic ∇EMG. **b**, Time-course of kainic-acid-induced whisking. Instantaneous peak-to-peak amplitude (top) and frequency (bottom) of vibrissa motion (blue) and frequency of breathing (red). The animal starts to wake by 100 min. **c**, Polar plots of the coherence between spiking activity and vibrissa motion at the peak frequency of whisking (8.8 Hz median); only units with statistically significant coherence (32 of 33 units, $P < 0.01$) are shown. Open circles represent multi-unit activity and closed circles represent single units. The green bar represents the coherence of the ∇EMG for the intrinsic muscle (panel **a**) with vibrissa motion. (Inserts) Spiking activity of neuronal units in the vIRt (black) in relation to vibrissa motion (blue). **d**, One of the locations that corresponded to a unit in panel **c**, labelled via iontophoretic injection of neurobiotin through the recording electrode. **e**, Axons (yellow arrowheads) and terminals in the ventral lateral division of the facial nucleus after neurobiotin injection at the recording site in panel **d**. **f**, Three-dimensional reconstruction of the labelled recording locations for the units in panel **c**.

with protraction, as in the case of units identified during intervening whisks in the behaving animal (Fig. 3c–f), as well as units that spiked in anti-phase (32 units for four rats) (Fig. 4c). Microinjection of neurobiotin at the recording site (Fig. 4d) resulted in anterograde labelling of axon terminals in the ventrolateral part of the facial nucleus, where motor neurons that innervate the intrinsic muscles are clustered (Fig. 4e). The recording sites were located medial to the ambiguus nucleus (Fig. 4f), similar to the region localized by recording in behaving animals (Fig. 3d, e).

Lesion of the vIRt abolishes ipsilateral whisking

The above results provide evidence for the sufficiency of neurons in the vIRt to drive rhythmic protraction. We next considered the necessity of the vIRt for rhythmic motion, and tested whether a lesion to this zone suppresses whisking. First, small electrolytic lesions of the IRt medial to the ambiguus nucleus abolish whisking on the side of the lesion, whereas whisking persists on the contralateral side (Fig. 5a–c and Supplementary Video 2). Neither basal respiration nor sniffing is affected by the lesion. Furthermore, the suppression of whisking seemed to be permanent as no recovery was observed up to 10 days after the lesion. Qualitatively similar results were found with ibotenic acid or Sindbis viral lesions (Supplementary Fig. 11), which indicates that the abolition of whisking is not attributable to severed axons of passage.

The spatial specificity of the ablations was assessed by lesioning various regions in the pons and medulla in a number of animals (head-fixed, three electrolytic; free-ranging, 16 electrolytic, 1 ibotenic acid, and 5 Sindbis). Lesions made in the dorsal part of IRt, in the parvocellular reticular formation, in the paragigantocellular reticular formation, or in the caudal part of the medullary reticular formation excluding the pre-Bötzinger complex, only minimally affected whisking (Fig. 5d–f). Critically, lesions within the vIRt that were as small as 200 μm in diameter were sufficient to severely impair whisking on the

ipsilateral side. We conclude that units in the vIRt have an obligatory role in the generation of whisking.

Anatomy of the circuit for rhythmic whisking

The behavioural (Figs 1 and 2) and physiological data (Figs 3–5) suggest that cells in inspiratory nuclei reset an oscillatory network of whisking units in the vIRt that can drive protraction of the vibrissa concurrent with each inspiration. We used tract-tracing methods to assess this proposed connection. Injections of biotinylated dextran amine (BDA) into the pre-Bötzinger complex, identified by the phase relation of units relative to breathing (two rats), led to dense anterograde labelling in the IRt medial to the ambiguus nucleus, including a number of axon terminals (Fig. 6a). This corresponds to the same region in which we observed whisking units (Figs 3d, e and 4d, f) and in which lesions extinguished ipsilateral whisking (Fig. 5e, f). These results support a direct connection from the pre-Bötzinger complex to the vIRt.

We next delineated the projections from neurons in the vIRt to facial motor neurons (Fig. 4d, e). Neurobiotin (three rats) or Fluorogold (two rats) was injected in the lateral aspect of the facial nucleus (Figs 6b and Supplementary Fig. 12). We observed a cluster of retrogradely labelled cells in the IRt that lie medial to the ambiguus nucleus (Fig. 6b). A detailed map of the location of cells that were retrogradely labelled from an injection in the lateral aspect of the facial nucleus (1,300 cells in one rat) reveals a rostrocaudal band of cells in the IRt; we identify this region as vIRt (Fig. 6c and Supplementary Fig. 12). Together, these and previous[26,27] patterns of neuronal labelling in the IRt support a direct connection from the vIRt to the facial nucleus and substantiate the role of the vIRt as a premotor nucleus.

The neurotransmitter content of neurons in the vIRt that project to the facial motor neurons was assessed by the combination of retrograde labelling and *in situ* hybridization[28] (Supplementary Figs 13 and 14). We find a fractional contribution of 0.12 ± 0.02 (mean $\pm$ s.e.m.; 259 cells in 3 rats) glutamatergic, 0.85 ± 0.02 (303 cells) glycinergic, and 0.53 ± 0.03 (237 cells) GABAergic neurons. These data support either monosynaptic excitatory transmission through glutamate receptors and through glycine NR3b receptors[29], or monosynaptic inhibitory transmission through glycine and GABA receptors in the presence of a tonic excitatory drive.

The involvement of the nasolabialis muscle during inspiratory whisks, but not intervening whisks, suggests that retraction of the mystacial pad is controlled by units in the Bötzinger or parafacial complex (Figs 2c and 3b). These units are phase-locked with expiration (Fig. 3d–f). The Bötzinger and parafacial region is in close proximity to the facial nucleus[1] and is reported to modulate the activity of facial motor neurons[18,30] that drive the nasolabialis muscle[31]. In support of a direct connection from the Bötzinger complex to facial motor neurons, we observed that the map of retrogradely labelled projections to the facial nucleus shows strong labelling (Fig. 6c). In addition, small injections of neurobiotin that were made in the parafacial region (three rats) (Fig. 6d) labelled axon terminals specifically in the dorsolateral part of the facial nucleus, where motor neurons that innervate the extrinsic muscles are clustered. This result supports the conclusion that retraction of the vibrissae is at least partly mediated by neurons in the Bötzinger or parafacial region.

Discussion

We have identified units in a newly defined zone of the intermediate band of the reticular formation in the medulla, the vIRt, that oscillate in phase with motion of the vibrissae (Fig. 7a). This zone functions as the premotor pattern generator for rhythmic whisking and is part of a larger circuit in which cells in nuclei that are obligatory for inspiration[11,32,33] reset the phase of vIRt units with each breath (Fig. 7b). Thus, whisking during sniffing is effectively driven on a cycle-by-cycle basis by the inspiratory rhythm generator, whereas intervening whisks between successive inspirations result from oscillations of the
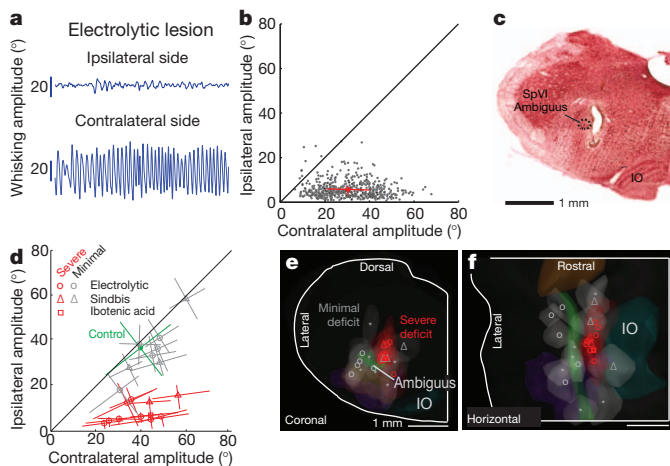

Figure 5 | Lesion of the vIRt impairs ipsilateral whisking. a, An example of a whisking bout after an electrolytic lesion. **b**, A scatter plot of ipsilateral versus contralateral whisk amplitudes reveals the functional completeness of the lesion; each dot represents one whisk, the red cross represents the mean, and red lines represent the inter-quartile range. **c**, Histological analysis confirms that the lesion is in the vIRt; coronal section stained with neutral red. SpVI, interpolaris division of the spinal trigeminal complex. **d**, Composite results for a subset of lesions (19 rats) for which vibrissa position was tracked; lines are central quartiles. Symbols correspond to the method of lesion. Results were scored by the severity of the ipsilateral whisking deficit: severe, greater than 50% reduction (as in panels **a** and **b**), or minimal, less than 50% reduction. Whisking of a non-lesioned control rat is shown in green. **e, f**, Lesion sites were mapped onto a three-dimensional reconstruction of the medulla and selected anatomical substructures (as in Fig. 4f). The lesion centroids are denoted with the symbols in panel **d** and have a median volume of 0.2 μl. Sites marked with an asterisk (six rats) represent additional lesions (not shown in panel **d**) that resulted in minimal whisking deficits as assessed by visual inspection. White lines are tissue boundaries or limits of the reconstruction.
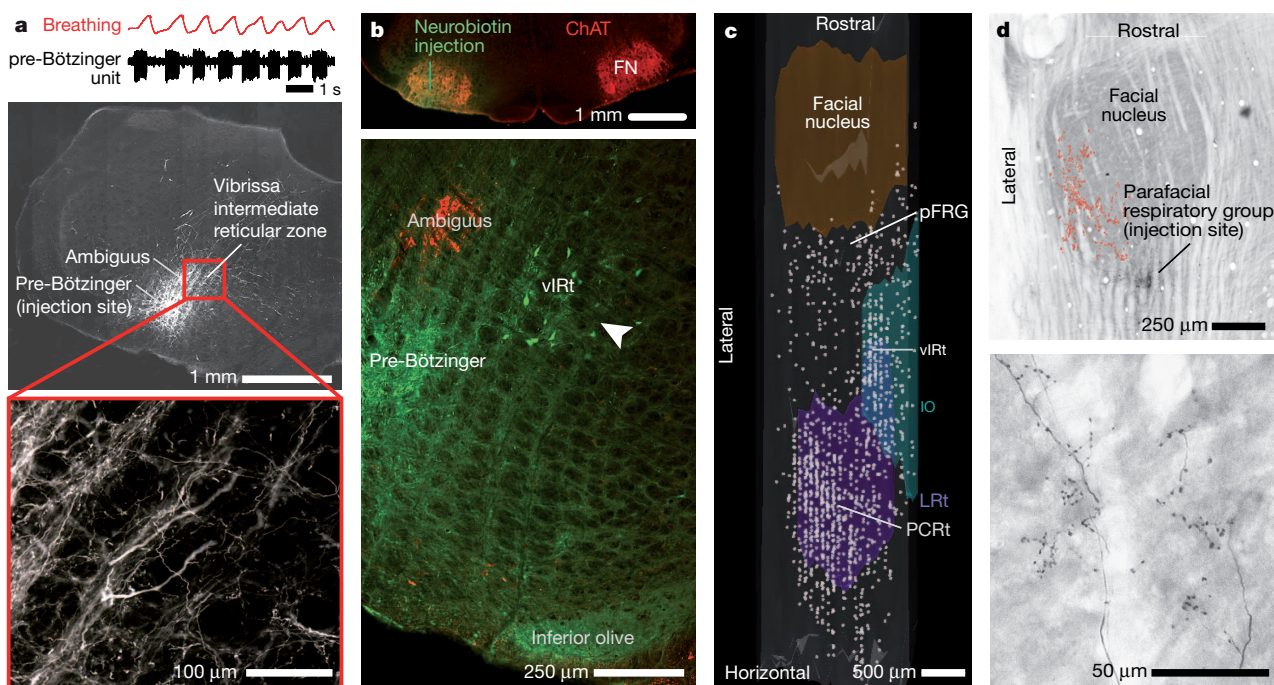
Figure 6 | Anatomical evidence for connections between respiratory and whisking zones. a, Recording of a single inspiratory unit in the pre-Bötzinger complex, together with breathing (top). Injection of biotinylated dextran amine through the same pipette (middle) leads to anterograde labelling of axons and terminals in the vIRt (bottom); middle and bottom panels are coronal sections. **b**, Injection of neurobiotin (green) into the facial nucleus (FN) (top) retrogradely labels neurons in the vIRt (bottom; white arrowhead). Labelling with α-choline acetyl-transferase (ChAT) highlights motor neurons in the facial and ambiguus nuclei (red). **c**, The locations of cells that were retrogradely labelled from the facial nucleus with neurobiotin, superimposed on a

three-dimensional reconstruction of the medulla. Note the labelled cells in the vIRt, located between coronal planes −12.5 and −13.0 mm relative to bregma, that span approximately 200 μm along the lateral–medial axis. PCRt, parvocellular reticular nucleus; pFRG, the parafacial respiratory group. **d**, Injection of neurobiotin into the parafacial region labels terminals in the dorsolateral aspect of the facial nucleus (top). Individual axons and terminals are seen in the bottom panel, and a compendium across three consecutive sections is summarized in the top panel (red dots). Horizontal sections were stained for cytochrome oxidase.

whisking units in the vIRt. Retraction of the vibrissae by extrinsic muscles in the mystacial pad is probably controlled by nuclei that lie immediately caudal to the facial nucleus and that are active during expiration.

Our results may be relevant to the generation of other rhythmic orofacial behaviours, for which licking is particularly well described. First, tongue protrusions are coordinated with the respiratory cycle[34]. Second, the hypoglossal premotor neurons are concentrated in the IRt, dorsomedial to the pre-Bötzinger complex[3,35], and are driven by

bursts of spikes that are locked to inspiration[36]. Third, the output of units in the hypoglossal IRt zone locks to rhythmic licking[37]. Finally, infusion of an inhibitory agonist into the IRt blocks licking[38]. These past results are consistent with a model in which pre-Bötzinger units reset the phase of bursting in a network of hypoglossal premotor neurons in the IRt zone, in parallel with our circuit for whisking (Fig. 7b). Serotonergic and other modulatory inputs may serve to gate and accelerate all of these rhythms[39–43].
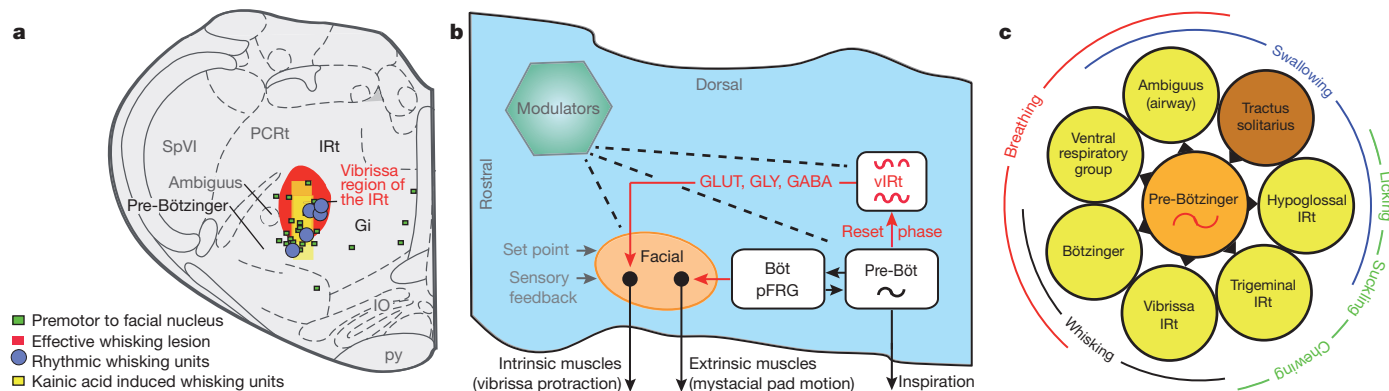

Figure 7 | The whisking rhythm generator circuit in the broader context of orofacial behaviours. a, Summary of evidence for a rhythm generator in the vibrissa zone of the intermediate band of the reticular formation (IRt; grey). This region contains units that fire in phase with all whisking events in freely behaving animals as well as when whisking is induced by microinjection of kainic acid. This region also contains cells that project to the facial nucleus, and lesions of this area severely disable whisking on the ipsilateral side. Gi, gigantocellular reticular formation; py, pyramidal tract. **b**, Model of the

medullary circuitry that generates whisking in coordination with breathing. Red lines indicate new findings from this work. Dashed lines indicate diffuse synaptic input from modulatory brain nuclei. GLUT, glutamate; GLY, glycine; GABA, γ-aminobutyric acid. **c**, Summary of all premotor nuclei (yellow) that are known to receive rhythmic drive from the pre-Bötzinger complex (orange), or conjectured to receive input based on anatomical projections, along with a potential resetting circuit (brown). The nuclei serve shared oral facial behaviours, as shown here for whisking (black) and breathing (red).

The common architecture of the control circuits for whisking (Fig. 7b) and licking[3] supports the primary role of breathing in the coordination of orofacial behaviours. In the absence of interruptions, such as from swallowing[44] or aversive stimuli[19], we propose that the inspiratory pattern generator broadcasts a master clock signal to the various patterning circuits throughout the IRt and nearby zones (Fig. 7c). Coordination by this breathing clock can ensure that these rhythmic behaviours, which share muscle groups, do not confound each other. It is also possible that the breathing clock serves as a phase-locking rhythmic signature to bind the perception of olfactory and tactile inputs.

METHODS SUMMARY

All procedures are in accordance with the Institutional Animal Care and Use Committee guidelines of the home institute of each investigator. Thirty-seven female Long Evans rats were used for behavioural and electrophysiological experiments, an additional 25 Long Evans rats of mixed sex were used solely for lesion studies, and 10 female Long Evans and 3 male Sprague Dawley rats were used for anatomical studies. Recording, labelling, anatomy and *in situ* hybridization were carried out using longstanding methods[25,28,45] but with refinements.

Full Methods and any associated references are available in the online version of the paper.

1. Smith, J. C., Abdala, A. P. L., Rybak, I. A. & Paton, J. F. R. Structural and functional architecture of respiratory networks in the mammalian brainstem. *Phil. Trans. R. Soc. B* **364**, 2577–2587 (2009).
2. Nakamura, Y. & Katakura, N. Generation of masticatory rhythm in the brainstem. *Neurosci. Res.* **23**, 1–19 (1995).
3. Travers, J. B., Dinardo, L. A. & Karimnamazi, H. Motor and premotor mechanisms of licking. *Neurosci. Biobehav. Rev.* **21**, 631–647 (1997).
4. Alheid, G. F. & McCrimmon, D. R. The chemical neuroanatomy of breathing. *Respir. Physiol. Neurobiol.* **164**, 3–11 (2008).
5. Feldman, J. L., Del Negro, C. A. & Gray, P. A. Understanding the rhythm of breathing: so near, yet so far. *Annu. Rev. Physiol.* **75**, 423–452 (2013).
6. Garcia, A. J., Zanella, S., Koch, H., Doi, A. & Ramirez, J. M. Networks within networks: the neuronal control of breathing. *Prog. Brain Res.* **188**, 31–50 (2011).
7. Welker, W. I. Analysis of sniffing of the albino rat. *Behaviour* **22**, 223–244 (1964).
8. Brecht, M. & Freiwald, W. A. The many facets of facial interactions in mammals. *Curr. Opin. Neurobiol.* **22**, 259–266 (2011).
9. Vincent, S. B. The function of the vibrissae in the behavior of the white rat. *Behavior Monographs* **1**, 7–81 (1912).
10. Smith, J. C., Ellenberger, H. H., Ballanyi, K., Richter, D. W. & Feldman, J. L. Pre-Botzinger complex: a brainstem region that may generate respiratory rhythm in mammals. *Science* **254**, 726–729 (1991).
11. Tan, W. et al. Silencing preBötzinger complex somatostatin-expressing neurons induces persistent apnea in awake rat. *Nature Neurosci.* **11**, 538–540 (2008).
12. Dobbins, E. G. & Feldman, J. L. Brainstem network controlling descending drive to phrenic motoneurons in rat. *J. Comp. Neurol.* **347**, 64–86 (1994).
13. Bieger, D. & Hopkins, D. A. Viscerotopic representation of the upper alimentary tract in the medulla oblongata in the rat: the nucleus ambiguus. *J. Comp. Neurol.* **262**, 546–562 (1987).
14. Semba, K. & Komisaruk, B. R. Neural substrates of two different rhythmical vibrissal movements in the rat. *Neuroscience* **12**, 761–774 (1984).
15. Berg, R. W. & Kleinfeld, D. Rhythmic whisking by rat: retraction as well as protraction of the vibrissae is under active muscular control. *J. Neurophysiol.* **89**, 104–117 (2003).
16. Gao, P., Bermejo, R. & Zeigler, H. P. Vibrissa deafferentation and rodent whisking patterns: behavioral evidence for a central pattern generator. *J. Neurosci.* **21**, 5374–5380 (2001).
17. Huangfu, D., Koshiya, N. & Guyenet, P. G. Central respiratory modulation of facial motoneurons in rats. *Neurosci. Lett.* **151**, 224–228 (1993).
18. Onimaru, H., Kumagawa, Y. & Homma, I. Respiration-related rhythmic activity in the rostral medulla of newborn rats. *J. Neurophysiol.* **96**, 55–61 (2006).
19. Lawson, E. E., Richter, D. W., Czyzyk-Krzeska, M. F., Bischoff, A. & Rudesill, R. C. Respiratory neuronal activity during apnea and other breathing patterns induced by laryngeal stimulation. *J. Appl. Ohysiology* **70**, 2742–2749 (1991).
20. Fukuda, Y. & Honda, Y. Differences in respiratory neural activities between vagal (superior laryngeal), hypoglossal, and phrenic nerves in the anesthetized rat. *Jpn. J. Physiol.* **32**, 387–398 (1982).
21. Ermentrout, G. B. & Kleinfeld, D. Traveling electrical waves in cortex: insights from phase dynamics and speculation on a computational role. *Neuron* **29**, 33–44 (2001).
22. Sherrey, J. H. & Megirian, D. State dependence of upper airway respiratory motoneurons: functions of the cricothyroid and nasolabial muscles of the unanesthetized rat. *Electroencephalogr. Clin. Neurophysiol.* **43**, 218–228 (1977).
23. Haidarliu, S., Golomb, D., Kleinfeld, D. & Ahissar, E. Dorsorostral snout muscles in the rat subserve coordinated movement for whisking and sniffing. *Anat. Rec.* **295**, 1181–1191 (2012).
24. Dörfl, J. The musculature of the mystacial vibrissae of the white mouse. *J. Anat.* **135**, 147–154 (1982).
25. Hill, D. N., Bermejo, R., Zeigler, H. P. & Kleinfeld, D. Biomechanics of the vibrissa motor plant in rat: rhythmic whisking consists of triphasic neuromuscular activity. *J. Neurosci.* **28**, 3438–3455 (2008).
26. Takatoh, J. et al. New modules are added to vibrissal premotor circuitry with the emergence of exploratory whisking. *Neuron* **77**, 346–360 (2013).
27. Isokawa-Akesson, M. & Komisaruk, B. R. Difference in projections to the lateral and medial facial nucleus: anatomically separate pathways for rhythmical vibrissa movement in rats. *Exp. Brain Res.* **65**, 385–398 (1987).
28. Furuta, T. et al. Inhibitory gating of vibrissal inputs in the brainstem. *J. Neurosci.* **28**, 1789–1797 (2008).
29. Chatterton, J. E. et al. Excitatory glycine receptors containing the NR3 family of NMDA receptor subunits. *Nature* **415**, 793–798 (2002).
30. Pagliardini, S. et al. Active expiration induced by excitation of ventral medulla in adult anesthetized rats. *J. Neurosci.* **31**, 2895–2905 (2011).
31. Klein, B. G. & Rhoades, R. The representation of whisker follicle intrinsic musculature in the facial motor nucleus of the rat. *J. Comp. Neurol.* **232**, 55–69 (1985).
32. Gray, P. A. et al. Developmental origin of preBötzinger complex respiratory neurons. *J. Neurosci.* **30**, 14883–14895 (2010).
33. Bouvier, J. et al. Hindbrain interneurons and axon guidance signaling critical for breathing. *Nature Neurosci.* **13**, 1066–1074 (2010).
34. Welzl, H. & Bures, J. Lick-synchronized breathing in rats. *Physiol. Behav.* **18**, 751–753 (1977).
35. Koizumi, H. et al. Functional imaging, spatial reconstruction, and biophysical analysis of a respiratory motor circuit isolated *in vitro*. *J. Neurosci.* **28**, 2353–2365 (2008).
36. Ono, T., Ishiwata, Y., Inaba, N., Kuroda, T. & Nakamura, Y. Modulation of the inspiratory-related activity of hypoglossal premotor neurons during ingestion and rejection in the decerebrate cat. *J. Neurophysiol.* **80**, 48–58 (1998).
37. Travers, J. B., DiNardo, L. A. & Karimnamazi, H. Medullary reticular formation activity during ingestion and rejection in the awake rat. *Exp. Brain Res.* **130**, 78–92 (2000).
38. Chen, Z., Travers, S. P. & Travers, J. B. Muscimol infusions in the brain stem reticular formation reversibly block ingestion in the awake rat. *Am. J. Physiol. Regul. Integr. Comp. Physiol.* **280**, R1085–R1094 (2001).
39. DePuy, S. D., Kanbar, R., Coates, M. B., Stornetta, R. L. & Guyenet, P. G. Control of breathing by raphe obscurus serotonergic neurons in mice. *J. Neurosci.* **31**, 1981–1990 (2011).
40. Doi, A. & Ramirez, J. M. Neuromodulation and the orchestration of the respiratory rhythm. *Respir. Physiol. Neurobiol.* **164**, 96–104 (2008).
41. Hattox, A., Li, Y. & Keller, A. Serotonin regulates rhythmic whisking. *Neuron* **39**, 343–352 (2003).
42. VanderMaelen, C. P. & Aghajanian, G. K. Intracellular studies showing modulation of facial motoneurone excitability by serotonin. *Nature* **287**, 346–347 (1980).
43. Harish, O. & Golomb, D. Control of the firing patterns of vibrissa motoneurons by modulatory and phasic synaptic inputs: a modeling study. *J. Neurophysiol.* **103**, 2684–2699 (2010).
44. Saito, Y., Ezure, K., Tanaka, I. & Osawa, M. Activity of neurons in ventrolateral respiratory groups during swallowing in decerebrate rats. *Brain Dev.* **25**, 338–345 (2003).
45. Kleinfeld, D., Sachdev, R. N. S., Merchant, L. M., Jarvis, M. R. & Ebner, F. F. Adaptive filtering of vibrissa input in motor cortex of rat. *Neuron* **34**, 1021–1034 (2002).

Author Contributions M.D., D.K. and J.D.M. planned the experiments and wrote the manuscript. M.D., T.F. and J.D.M. carried out the rat experiments with assistance from M.D. for the histology and vibrissae tracking. D.H. carried out the mouse experiments with surgical assistance from M.C.S. Data analysis was carried out by J.D.M. with methodological contributions from D.K.

Author Information Reprints and permissions information is available at www.nature.com/reprints. The authors declare no competing financial interests. Readers are welcome to comment on the online version of the paper. Correspondence and requests for materials should be addressed to M.D. (martin.deschenes@crulrg.ulaval.ca) or D.K. (dk@physics.ucsd.edu).

METHODS

Animals. Thirty-seven female Long Evans rats (250 to 350 g, Charles River) were used for behavioural and electrophysiological experiments, an additional 25 Long Evans rats of mixed sex were used solely for lesion studies, and 10 female Long Evans and 3 male Sprague Dawley rats were used for anatomical studies. Four adult mice, two male C57BL/6J and two female ChR2-MBD[46] mice were used for behavioural studies. Experimental protocols were carried out in accordance with federally prescribed animal care and use guidelines and were approved by the Institutional Animal Care and Use Committees at the University of California in San Diego, Laval University, Kyoto University, and the Janelia Farms Research Center.

Preparation. Head-fixed rats were habituated to body restraint for 5 days, then implanted with a custom-built head restraining mount[45] and a thermocouple (K-type; Omega Engineering) in the nasal cavity[47]. Surgical procedures were carried out in animals anaesthetized with ketamine (90 mg kg^{-1}) and xylazine (5 mg kg^{-1}). In brief, a craniotomy was performed over the cerebellum, and a plastic chamber was centred over the opening and secured with acrylic cement. The craniotomy was filled with silicone gel (no. 3-4689; Dow Corning). In two animals, Teflon-coated tungsten wires were inserted in the vibrissa pad to record activity of the intrinsic muscles and of the nasolabialis muscle[15,25]. Rats were allowed to recover for 2 days before the onset of behavioural experiments. During the recording sessions, rats were placed inside a body-restraining cloth sack and rigid tube, and the animals were head-restrained[45]. All vibrissae except C2 or D2 were cut at the base and movement of the intact vibrissa was recorded with videography. Rats were coaxed to whisk by presenting food or bedding from the home cage[48]. Finally, in some experiments, a tube was placed in front of the snout to deliver one or two 2-s puffs of air saturated with ammonia while the animal whisked.

Head-fixed mice were implanted with a titanium bar for head fixation[49] and with a stainless steel cannula to measure breathing, as described previously[50]. The mice were allowed to recover for 10 days before behavioural experiments.

Recording and analysis. To measure whisking, vibrissa motion in head-fixed rats was monitored in one of several ways with a Basler A602f camera at a spatial resolution of 120 µm per pixel or an NMOS linear sensor (S3904-2048Q; Hamamatsu). For behavioural measurements, 360 × 250 pixel planar images were acquired at 250 Hz with a white light emitting diode backlight for trials of 10 s each. Vibrissa angle was tracked by fitting a line to the spatially contiguous pixels comprising the initial 5 mm segment of the vibrissa base. For measurements in conjunction with extracellular recording from brainstem, we used either the Basler A602f camera in line-scan mode with a 1-kHz scan rate or the NMOS linear sensor and imaged motion along a line that was 5 to 10 mm from the edge of the mystacial pad. Pixel intensity along the line was thresholded and the centroid of the detected vibrissa was converted to a voltage proportional to pixel position in real time.

Vibrissa motion in freely moving rats with one or more vibrissae in the C or D row was monitored with a HiSpec 2G Mono camera (Fastec Imaging) at a 250-Hz frame rate, or a Powershot SX260HS camera at a 120-Hz frame rate (Canon). Rats were placed in a raised, clear plastic box with a passageway that allowed them to perch in search of their home cage, located 20 cm away. Trained animals craned across the gap and sniffed and whisked vigorously[48]. Vibrissa motion was tracked with commercial software (ProAnalyst, Xcitex), and previously described algorithms[51].

Vibrissa motion in head-fixed mice with vibrissae in the C row was recorded with a high-speed CMOS camera (EOSENS CL; Mikrotron) through a telecentric lens (×0.36; Edmund Optics). Streampix 3 software (Norpix) was used to acquire the images, 640 × 352 pixels at a spatial resolution of 24 µm per pixel. The vibrissae were illuminated from below with collimated infrared light from a high-power light emitting diode (640nm; Roithner). Vibrissa motion was tracked with automated procedures[49].

The extracted vibrissa movements for all cases were separated into single whisks by band-pass filtering the position traces between 3 and 25 Hz with a 3-pole Butterworth filter run in forwards and backwards directions, and applying the Hilbert transform[52]. Individual candidate whisks were identified by phase resets of the Hilbert transform, and were accepted only if the minimum-to-maximum amplitude exceeded 5° and the whisk lasted less than 250 ms. The onset time of each whisk was defined as the time at which the vibrissa angle exceeded 10% of the minimum-to-maximum amplitude.

For electromyography, muscular activity was monitored in different muscle groups, and the integrated envelope of the EMG activity, denoted |∇EMG|, was computed as described previously[15,25]. We then computed the cross-correlation between protraction onset times and the |∇EMG|. The 95% confidence intervals were obtained by 1,000 re-samples from the set of protraction onset times and computing the cross-correlation with the re-sampled data set.

To measure breathing, respiration-related changes in temperature or pressure sensors were digitized and band-pass filtered between 1 and 15 Hz with a 3-pole Butterworth filter run backwards and forwards in time. Onset times for inspiratory events were defined as described above for whisking.

In rats, respiration-related changes in temperature were verified to be synchronous with chest expansion, which are presumed to track diaphragm movements, as measured with a piezoelectric strap around the abdomen in separate experiments.

To examine neuronal signalling in awake, behaving rats, multi-unit neuronal activity was recorded in the ventral medulla with quartz micropipettes, with a tip diameter of 10 to 25 µm, filled with 2% (w/v) Chicago sky blue (Sigma) in artificial cerebral spinal saline, or with tungsten microelectrodes (1 MΩ impedance; Microprobes). Electrode position was controlled by a motorized manipulator (model MP-285, Sutter). Units were held for 1 to 20 min. Signals were amplified, band-pass filtered between 300 Hz and 6 kHz and sampled at 20 or 40 kHz. The noise level, σ, was defined as the standard deviation of the voltages recorded over the entire time that the electrode was maintained at a recording site. Multi-unit spike events were defined as voltage fluctuations that exceeded 3.5 times σ.

One or more recording sites in each session were marked with an extracellular deposit of Chicago sky blue by electrophoresis; −10 to −50 µA with 10-s pulses spaced every 20 s for 5 min, or by electrolytic lesion with 40 to 80 µA applied for three intervals of 2 to 5 s. Rats were deeply anaesthetized at the end of the session and perfused with phosphate buffered saline (PBS), and then with 4% (w/v) paraformaldehyde in PBS. Brains were post-fixed overnight in 4% paraformaldehyde in PBS, cryoprotected in 30% (w/v) sucrose in PBS, and sectioned along the sagittal or coronal plane at a thickness of 60 µm with a freezing microtome. Sections were stained with either Neutral red, Neurotrace blue (fluorescent Nissl; Invitrogen) or cytochrome oxidase[53].

To investigate kainic acid-induced whisking, microinjections of kainic acid were made through quartz or glass micropipettes, 10 to 15 µm in diameter, in rats that were anaesthetized with ketamine and xylazine as described above. Injections were targeted to the approximate vibrissa region of the intermediate band of the reticular formation (vIRt) as defined in our anatomical studies (Fig. 6) using stereotaxic coordinates. Kainic acid was prepared as 1% (w/v) in Tris buffer, pH 8.2, and delivered by iontophoresis with −500 nA, 250-ms pulses spaced every 500 ms for 600 s. In several experiments, biotinylated dextran amine (M_r 3000; Invitrogen) prepared as 2% (w/v), was added to the solution to label the injection site.

Rats were secured with a head-fixed mount and their vibrissae were monitored with a camera in linescan mode (Basler A602f). Coordinated, rhythmic vibrissa movements typically began 15 to 30 min after the kainic acid injection, at which point all vibrissae except C2 or D2 were trimmed. Individual whisks were detected, as described above, with the exception that the threshold for detecting a whisk was set to 1°.

Single and multi-unit recordings in the vicinity of the site of the kainic acid injections were made in a subset of rats using glass microelectrodes with 2- to 3-µm tips back-filled with neurobiotin (Vector Labs), prepared as a 2% (w/v) solution in 500 mM potassium acetate. These pipettes served for both recording and labelling of the recording site. The centroid of injection sites that induced whisking varied by up to 1 mm relative to the actual anatomical location of the vIRt, consistent with variability in stereotaxic coordinates between rats[54] and the rapid diffusion of kainic acid. We thus made multiple penetrations offset from each other by at most 100 µm to locate units whose spiking was locked to whisking after the kainic acid injection. The depth of each unit along a penetration was noted, and at the end of a subset of the experiments the recording site was labelled by iontophoresis; +50 to +100 nA, 2-s pulses spaced every 4 s for 1,000 s. The animals were perfused 2 h after the injection.

For coherence and correlation analysis, we assessed the degree and statistical significance of correlation between whisking and breathing events (Fig. 1d) by computing the cross correlation between whisk onset times and breath onset times separately for basal respiration, with rates of less than 3 Hz, and sniffing, with rates of greater than 5 Hz. The maximum lag for the cross correlation computed in each case was bounded by the minimum breathing period. Statistical significance was assessed by performing a one sample Kolmogorov–Smirnov test versus the uniform distribution expected by chance. In accordance with this, we define the modulation depth of the cross correlation as the corresponding Kolmogorov–Smirnov test statistic.

Additional analyses were carried out in the frequency domain to assess the spectral content and synchrony between whisking, breathing and spiking activity. For experiments in awake animals, whose behaviour exhibited interleaved bouts of basal respiration, sniffing and whisking, our data were segmented as follows. First, 'inspiratory' whisks were defined as those whisks whose onset occurred within 100 ms of an inspiration, whereas intervening whisks were defined as whisks that did not occur within 100 ms of the closest onset of inspiration.

Next, behavioural epochs were classified as 'basal respiration' when the instantaneous respiratory frequency was less than 3 Hz, 'sniffing' for periods when the instantaneous respiratory frequency was greater than 5 Hz, 'inspiratory whisking' for periods of successive inspiratory whisks, and 'intervening whisking' for periods of successive intervening whisks during 'basal respiration'. Bouts of these behaviours were divided into non-overlapping segments of a pre-determined length; that is, 1 s for basal respiration, 500 ms for sniffing and inspiratory whisking, and 300 ms for intervening whisking. For each segment, we extracted the relevant behavioural signal; that is, inspiration onset times for basal respiration and sniffing, and vibrissa position for inspiratory and intervening whisking, and the relevant physiological signal (the $|\nabla EMG|$ or the multi-unit spike times).

The Chronux toolbox (http://www.chronux.org) was used to compute the spectral coherence between these respective behavioural and physiological signals, averaged over all segments with a time-bandwidth product of one. We report the magnitude and phase of the coherence at the peak frequency of the behaviour (Fig. 1c); that is, 2 Hz for basal respiration, 6 Hz for sniffing and inspiratory whisking, and 8 Hz for intervening whisking. The whisking and breathing analyses are normalized so that a phase of zero corresponds to the onsets of protraction and inspiration, respectively, as defined above.

For experiments in anaesthetized animals with pharmacologically induced whisking, we computed the spectral coherence between vibrissa position and either spike times or $|\nabla EMG|$ irrespective of breathing, averaged over all 2-s segments with a time-bandwidth product of two. We report the magnitude and phase of the coherence at the peak frequency whisking, which varied between experiments. The analysis is normalized as above. Phase zero corresponds to the onset of protraction.

Medullary lesions and whisking. Electrolytic lesions were made with metal microelectrodes (0.5 MΩ; FHC) by passing direct current of +40 to +80 μA for 5 s at multiple nearby spatial locations. In select cases the lesions were performed with glass pipettes in head-fixed animals immediately after unit recordings in the vIRt. Ibotenic acid lesions were made by pressure injection of approximately 300 nl of ibotenic acid, prepared as 1% (w/v) in physiological saline. Sindbis virus lesions were made by pressure injection of approximately 100 to 300 nl of viral vector[55] (approximately 3×10^3 infectious particles per μl) using glass micropipettes with tips 30 μm in diameter. Two to five days after the animal recovered from surgery, high-speed videography of vibrissa motion was carried out on both sides of the face in both head-fixed and freely moving animals. Vibrissae were tracked and individual whisks were identified based on the motion on the contralateral side, as described above. The mean amplitude of the Hilbert transform over the period of each whisk was calculated for both the ipsilateral and contralateral sides.

Anatomy. For anterograde and retrograde labelling, all tracer injections were made under ketamine and xylazine anaesthesia, as above, with concurrent monitoring of respiration. Cells in the Bötzinger–parafacial complex were labelled with neurobiotin (Vector Labs), prepared as a 2% (w/v) solution in 500 mM potassium acetate. Glass microelectrodes with 4- to 5-μm tips served for both recording and injection. Bötzinger cells were identified by their expiration-related activity and neurobiotin was delivered by iontophoresis; +50 to +100 nA, 2-s pulses spaced every 4 s for 1,000 s. The animals were perfused after 90 min of recovery.

Cells in the pre-Bötzinger complex were similarly identified by their inspiration-related activity and labelled with biotinylated dextran amine (10 kDa molecular mass; Invitrogen), prepared as a 2% (w/v) solution in 500 mM potassium acetate. Biotinylated dextran amine was delivered by iontophoresis using glass microelectrodes with 8- to 10-μm tips; +200 nA, 2-s pulses spaced every 4 s for 1,000 s. The animals were perfused after 2 days of recovery.

Cells that projected to the facial motor nucleus were labelled retrogradely with neurobiotin, prepared as a 2% (w/v) solution in 10 mM sodium citrate buffer at pH 3.0 using glass microelectrodes with 20-μm tips. The location was confirmed by microstimulation, +5- to +10-μA pulses, 100 μs in width, delivered at 100 Hz, that led to movements of approximately 2° of one or more vibrissae. Neurobiotin was delivered by iontophoresis; +300 nA, 2-s pulses spaced every 4 s for 1,000 s. The animals were perfused after 3 h of recovery. Complementary studies involved the use of Fluorogold (Fluorochrome), prepared as a 1% (w/v) in 0.1 M cacodylate buffer at pH 7.0, delivered as above but with the animals perfused after 2 days.

After perfusion, brains were post-fixed for 2 h and cryoprotected in 30% (w/v) sucrose for 12 h. The brainstems were then isolated and cut in the coronal or

sagittal plane at a thickness of 50 μm on a freezing microtome. Neurobiotin and BDA were revealed with ABC Elite and SG kits (Vector Labs) or with streptavidin-Alexa 488 (1:200 dilution; Invitrogen). Fluorogold was revealed by immunohistochemistry (1:5,000 dilution; Millipore). Sections were then counterstained with Neutral red, immunostained for choline acetyltransferase (1:1,000 dilution of α-ChAt; Millipore), or reacted for cytochrome oxidase.

To examine lesion anatomy, animals lesioned with the Sindbis viral vector, for which we observed a severe deficit in whisking, were perfused immediately after video recordings; this corresponded to 50 to 75 h after injection of the virus. Animals that did not exhibit a deficit were perfused after 4 to 6 days. Animals lesioned electrolytically or with ibotenic acid were perfused 2 to 10 days after the procedure. For electrolytic lesions, 60-μm coronal or sagittal sections were stained for neutral red. For ibotenic acid and Sindbis viral lesions, 30 μm coronal or sagittal sections were immunostained for neuronal nuclear protein (1:200 dilution of anti-NeuN; Millipore). For Sindbis viral lesions, alternate sections were stained for myelin (Luxol fast blue; Sigma) and cell bodies (neutral red).

For mapping, histological sections were scanned at 1 μm spatial resolution using a Nanozoomer (Hamamatsu) digital slide scanner. The stereotaxic recording sites were superimposed on the scans according to their distance to the nearest labelled site. Sections containing Chicago sky blue deposits and associated recording sites were aligned by manual rotation and translation with an atlas of sagittal Nissl sections (brainmaps.org). The outlines of prominent medullary structures, including the facial nucleus, lateral reticular nucleus, nucleus ambiguus and inferior olive were traced with neurolucida (Microbrightfield) software, and sections were aligned based on these anatomical borders to yield a three-dimensional reconstruction of the medulla. The extents of brainstem lesions were similarly mapped onto standard frontal sections[56].

Combined anatomy and *in situ* hybridization. For retrograde labelling and *in situ* hybridization, tracer injections were made under ketamine and xylazine anaesthesia. Fluorogold, 4% (w/v) in saline, was injected into the lateral part of the facial nucleus by passing 500-nA current pulses, 7 s in duration, every 14 s for 300 s using glass microelectrodes with tips 20 μm in diameter. After a survival period of 48 h, rats were perfused as described above. After fixation, brains were removed, the brainstem isolated, cryoprotected with diethylpyrocarbonate-treated sucrose, and cut into 30-μm-thick sagittal sections on a freezing microtome for *in situ* hybridization[57].

To count cells, retrogradely labelled cells in sections processed for *in situ* hybridization were counted under confocal microscopy with a ×40 objective, as described[28]. Approximately ten fields were scanned in a grid-like manner across the vIRt, as defined in our other anatomical tracing experiments (Supplementary Fig. 8). For each field, a stack of 5 to 10 optical sections were acquired, and counts were made from the stacked images.

46. Lewis, T. L. Jr, Mao, T. & Svoboda, K. Myosin-dependent targeting of transmembrane proteins to neuronal dendrites. *Nature Neurosci.* **12,** 568–576 (2009).
47. Uchida, N. & Mainen, Z. F. Speed and accuracy of olfactory discrimination in the rat. *Nature Neurosci.* **6,** 1224–1229 (2003).
48. Ganguly, K. & Kleinfeld, D. Goal-directed whisking behavior increases phase-locking between vibrissa movement and electrical activity in primary sensory cortex in rat. *Proc. Natl Acad. Sci. USA* **101,** 12348–12353 (2004).
49. O'Connor, D. H. *et al.* Vibrissa-based object localization in head-fixed mice. *J. Neurosci.* **30,** 1947–1967 (2010).
50. Shusterman, R., Smear, M. C., Koulakov, A. A. & Rinberg, D. Precise olfactory responses tile the sniff cycle. *Nature Neurosci.* **14,** 1039–1044 (2011).
51. Knutsen, P. M., Derdikman, D. & Ahissar, E. Tracking whisker and head movements in unrestrained behaving rodents. *J. Neurophysiol.* **93,** 2294–2301 (2005).
52. Hill, D. N., Curtis, J. C., Moore, J. D. & Kleinfeld, D. Primary motor cortex reports efferent control of vibrissa position on multiple time scales. *Neuron* **72,** 344–356 (2011).
53. Deschênes, M., Timofeeva, E. & Lavallee, P. The relay of high frequency sensory signals in the whisker-to-barreloid pathway. *J. Neurosci.* **23,** 6778–6787 (2003).
54. Paxinos, G., Watson, C., Pennisi, M. & Topple, A. Bregma, lambda and the interaural midpoint in stereotaxic surgery with rats of different sex, strain and weight. *J. Neurosci. Methods* **13,** 139–143 (1985).
55. Ghosh, S. *et al.* Sensory maps in the olfactory cortex defined by long-range viral tracing of single neurons. *Nature* **472,** 217–220 (2011).
56. Paxinos, G. & Watson, C. *The Rat Brain in Stereotaxic Coordinates* 6th edn (Academic Press, 2007).
57. Ito, T. & Oliver, D. L. Origins of glutamatergic terminals in the inferior colliculus identified by retrograde transport and expression of VGLUT1 and VGLUT2 genes. *Front. Neuroanat.* **4,** 135 (2010).